

NRC Publications Archive Archives des publications du CNRC

Experimental investigations of an energy-efficient dynamic positioning controller for different sea conditions

Alagili, Osama; Fernando, Eranga; Ahmed, Salim; Imtiaz, Syed; Murrant, Kevin; Gash, Bob; Islam, Mohammed; Zaman, Hasanat

This publication could be one of several versions: author's original, accepted manuscript or the publisher's version. / La version de cette publication peut être l'une des suivantes : la version prépublication de l'auteur, la version acceptée du manuscrit ou la version de l'éditeur.

For the publisher's version, please access the DOI link below. / Pour consulter la version de l'éditeur, utilisez le lien DOI ci-dessous.

Publisher's version / Version de l'éditeur:

<https://doi.org/10.1016/j.oceaneng.2024.117297>

Ocean Engineering, 299, C, pp. 1-14, 2024-03-11

NRC Publications Archive Record / Notice des Archives des publications du CNRC :

<https://nrc-publications.canada.ca/eng/view/object/?id=c8d0de9d-607b-48c5-8668-4c911bd26c09>

<https://publications-cnrc.canada.ca/fra/voir/objet/?id=c8d0de9d-607b-48c5-8668-4c911bd26c09>

Access and use of this website and the material on it are subject to the Terms and Conditions set forth at

<https://nrc-publications.canada.ca/eng/copyright>

READ THESE TERMS AND CONDITIONS CAREFULLY BEFORE USING THIS WEBSITE.

L'accès à ce site Web et l'utilisation de son contenu sont assujettis aux conditions présentées dans le site

<https://publications-cnrc.canada.ca/fra/droits>

LISEZ CES CONDITIONS ATTENTIVEMENT AVANT D'UTILISER CE SITE WEB.

Questions? Contact the NRC Publications Archive team at

PublicationsArchive-ArchivesPublications@nrc-cnrc.gc.ca. If you wish to email the authors directly, please see the first page of the publication for their contact information.

Vous avez des questions? Nous pouvons vous aider. Pour communiquer directement avec un auteur, consultez la première page de la revue dans laquelle son article a été publié afin de trouver ses coordonnées. Si vous n'arrivez pas à les repérer, communiquez avec nous à PublicationsArchive-ArchivesPublications@nrc-cnrc.gc.ca.



Experimental investigations of an energy-efficient dynamic positioning controller for different sea conditions

Osama Alagili^a, Eranga Fernando^a, Salim Ahmed^a, Syed Imtiaz^{a,*}, Kevin Murrant^b, Bob Gash^b, Mohammed Islam^b, Hasanat Zaman^b

^a Faculty of Engineering and Applied Science, Memorial University of Newfoundland, 240 Queen Elizabeth Ave, St. John's, A1B3X5, NL, Canada

^b National Research Council, 1 Arctic Avenue, St. John's, A1B3T5, NL, Canada

ARTICLE INFO

Keywords:

Dynamic positioning
Control Algorithms
Nonlinear model predictive controller

ABSTRACT

The primary objective of a Dynamic Positioning (DP) controller is to maintain vessel position under varying environmental disturbances, while minimizing thruster usage. This work presents the development of an innovative energy-efficient DP controller, named Green NMPC (GNMPC), which minimizes thruster demand while upholding position constraints. Inspired from the structure of the economic nonlinear model predictive controller (ENMPC), GNMPC aligns with "green" objectives and performance metrics, notably thruster energy efficiency. Extensive DP tests were conducted across a spectrum of wave conditions, including head seas, oblique angles, and large position set-point changes, to validate the efficacy of the GNMPC approach and evaluate the dynamic positioning system's effectiveness in diverse challenging situations. The results demonstrated that the proposed controller is energy efficient compared to a benchmark NMPC and proportional-integral-derivative (PID) controller. It successfully reduced thruster demand in the sway direction compared to NMPC while preserving the vessel's positioning objectives.

1. Introduction

A dynamic positioning (DP) system keeps a ship at a designated position and desired heading using its thrusters (Fossen, 2002). DP technology is crucial in various applications, such as exploring deep-sea petroleum resources, off-shore supply operations, off-shore survey applications, etc. Accuracy, precision, and energy efficiency are key factors when designing and developing a DP system. In earlier studies, the main focus was on the accuracy and precision of the controller (Sorensen et al., 2002; Fannemel, 2008). In recent years, there has been a significant discussion on developing solutions prioritizing high efficiency and low carbon emissions. Improving efficiency within the DP system reduces carbon emissions during operation and mitigates the overall stress of components, enhancing their longevity. This study aims to implement and test popular DP control strategies, including one newly proposed energy-efficient DP controller, to compare performance and evaluate the efficiency and frequency of thruster movements.

The first DP systems developed in the 1960s used the standard proportional, inertial, derivative (PID) controllers for horizontal motion (surge, sway, and yaw). Tuning the gains of the PID controller to perform under various sea states is challenging. Various approaches have been reported in the literature for tuning PID controllers for DP. In a recent study, authors in Xu et al. (2020) proposed a fuzzy

rule based PID controller for DP applications, where the controller gains were obtained through fuzzy inference. Grimbale et al. (1980), Balchen et al. (1980), Saelid et al. (1983). Following the PID based DP controllers, more complex controllers based on modern control theory were introduced to DP application. Authors in Grimbale et al. (1980), Balchen et al. (1980) proposed an optimal control theory based DP controller with a Kalman filter based estimator to separate low frequency and high frequency motion of the vessel due to disturbances. Separating high and low frequency motions enabled the controllers to apply control actions only for low frequency motions due to forces such as wind, current and wave drift forces.

Another control strategy widely used in industry is model predictive control (MPC). A key feature of MPC is its ability to handle nonlinear and multi-input-multi-output system constraints. Early MPC-based DP systems utilized a linearized model of the vessel. The nonlinear dynamics of the vessel were linearized using the small angle theory (Wang, 2006). The vessel might deviate significantly from the operating point in practical DP applications. Hence, the assumptions made during linearization are violated, and the MPC might not provide the optimal control. Recent studies have proposed nonlinear model predictive controllers (NMPC) that utilize the vessel's nonlinear dynamics without linearization (Veksler et al., 2016; Du et al., 2016; Jayasiri et al., 2017).

* Corresponding author.

E-mail address: simtiiaz@mun.ca (S. Imtiaz).

<https://doi.org/10.1016/j.oceaneng.2024.117297>

Received 19 November 2023; Received in revised form 21 February 2024; Accepted 24 February 2024

Available online 11 March 2024

0029-8018/Crown Copyright © 2024 Published by Elsevier Ltd.

<http://creativecommons.org/licenses/by-nc-nd/4.0/>.

This is an open access article under the CC BY-NC-ND license

The control objectives of DP applications in literature have primarily aimed at maintaining the desired position and heading of the vessel. Continuously trying to correct the offset has often resulted in control demand that is large, erratic, and shortens the thrusters' life span. Several techniques have been proposed to minimize the variations in control demands. One such technique is to isolate the low frequency (LF) and high frequency (HF) motion of the vessel due to effect of waves using Kalman filter techniques and apply control based on the LF motion (Sørensen, 2011). In the similar line of work recently (Wei et al., 2022) proposed a control strategy called composite hierarchical anti-disturbance control (CHADC) integrating stochastic disturbance observer-based control (DOBC) theory, robust wave filter (RWF) method with H-infinity control. Other approaches minimize control demands artificially through imposing ramp rates, applying move accumulation, or using hysteresis switching to minimize back and forth switching of thrusters. An alternative approach is proposed by Kongsberg Inc. called "Green DP", which is an eco-conscious control system. Their system is designed to address excessive thruster activity, particularly in moderate environmental conditions, to decrease energy consumption, and provide an environmentally friendly solution. The Green DP controller has three main parts: the model predictive controller, the position predictor, and the environmental compensator. The system defines a working area inside the operational area, where the vessel can drift within. These areas are incorporated in the constraints and the cost function of the NMPC controller. The environmental compensator generates smooth attractive force towards the desired position, and the MPC generates more aggressive demands to prevent predicted overshoots. The authors claim that the combination of environmental compensator and MPC reduces dynamic thruster demands compared to a standard DP system. Hvamb (2001).

In line with the Green DP, we have successfully developed a controller whose structure is similar to an economic NMPC (ENMPC) (Grüne and Pannek, 2017). The developed controller does not incorporate the operational area in the constraints or in the cost function directly. Instead, the weights of the economic NMPC are defined as a function of the deviation from the desired position. Our achievement in building the controller has resulted in the reduction of DP's operational costs, particularly with regard to thruster demands, which in turn mitigates thruster wear and tear. We have transitioned costs related to an NMPC's setpoint tracking stage into economic costs within the optimization layer of our ENMPC. The controller was tested in a simulation environment and showed good promise (Alagili et al., 2022).

Table 1 presents a compilation of key studies on DP that have implemented various control strategies. Many studies have proposed a single controller without comparative evaluation against alternative controller types. Another observation is that most of the studies have used simulations to validate and compare the performance of the controllers. Very few experimental implementations of DP systems have been reported in the literature, and most of the experiments have taken place in open waters, mostly under calm conditions, where disturbances cannot be controlled. In contrast, our work focuses on conducting experiments in a controlled environment, allowing us to compare the performance of different controllers under various wave conditions. We seek to understand better how these controllers operate under specific settings and assess their efficacy in real-world scenarios by carefully controlling the experimental conditions.

This current research presents the implementation and experimental validation of the GNMPC proposed in Alagili et al. (2022). Experimental implementation of the controller poses many challenges: (i) the accuracy of the mathematical model developed using the first principle and 3D design was insufficient for the NMPC implementation. So, to get the model's parameters, we used system identification to get a more accurate estimation of model parameters. (ii) implementation in real-time requires a fast optimizer to solve the nonlinear minimization problem. The optimizer needs to converge within the sampling interval,

and (iii) data communication and implementation issues also need to be sorted for the experimental implementation.

The performance of the GNMPC is compared with a PID based DP controller and NMPC based DP controller. To the best of the authors' knowledge, this is the first study that has experimentally compared the performance of three different DP controllers under different sea conditions. We tested each controller under four different sea conditions: Sea with no waves (NW), regular waves (RW), irregular waves (IRW), and white noise waves (WNW). We conducted three types of tests to analyze the performance of the controllers properly: Station keeping in head seas, station keeping at oblique angles, and large position setpoint change.

The structure of this paper is as follows. The mathematical model of the vessel used in the NMPC is described in Section 2. The formulation of the GNMPC controller is discussed in Section 3. The experimental setup and the implementation details of the wave filter, communication, and controller are presented in Section 4. Section 5 presents the experimental results and comparison of the PID, NMPC, and GNMPC controllers. Finally, the findings and conclusion of the experiments are discussed in Section 6.

2. Mathematical modeling of vessel

A vessel floating freely in 3D space can move in six degrees of freedom (DOF). Fig. 1 shows the 6 DOF of the vessel and coordinate frames used in this paper. In DP applications, the main focus is to control the three motions: surge, sway, and heading. Therefore, a simplified vessel model with three DOF is defined as in Eq. (1), and Eq. (3) (Jayasiri et al., 2017).

$$\dot{\eta} = J(\psi)v. \quad (1)$$

The 3DOF kinematics are shown in Eq. (1), where $\eta = [x, y, \psi]^T$. $[x, y]$ is the horizontal position vector expressed in the inertial frame \mathcal{W} , and ψ is the heading of the vessel. The rotation matrix, $J(\psi) \in R^{3 \times 3}$, defines the rotation between the inertial and body frames and can be expressed as

$$J(\psi) = \begin{bmatrix} \cos(\psi) & -\sin(\psi) & 0 \\ \sin(\psi) & \cos(\psi) & 0 \\ 0 & 0 & 1 \end{bmatrix}. \quad (2)$$

The body-fixed surge velocity, sway velocity, and yaw rate are represented by $u, v, \text{ and } r$, respectively, and the body-fixed velocity vector is defined as $v = [u, v, r]^T$. The dynamics of the vessel are defined as follows.

$$(M_{RB} + M_A)\dot{v} + (C_{RB}(v) + C_A(v) + D(v))v = \tau, \quad (3)$$

where $M_{RB} \in R^{3 \times 3}$ and $M_A \in R^{3 \times 3}$ are the inertia matrices representing rigid body mass and the hydrodynamic added-mass.

$$M_{RB} = \begin{bmatrix} m & 0 & 0 \\ 0 & m & mx_G \\ 0 & mx_G & I_z \end{bmatrix}, \quad (4)$$

$$M_A = \begin{bmatrix} -X_{\dot{u}} & 0 & 0 \\ 0 & -Y_{\dot{v}} & -Y_{\dot{r}} \\ 0 & -N_{\dot{v}} & -N_{\dot{r}} \end{bmatrix}, \quad (5)$$

where m is the mass of the ship, I_z is the moment of inertia about the z axis, and x_G is the distance to the center of gravity of the ship along the x axis of the body frame B .

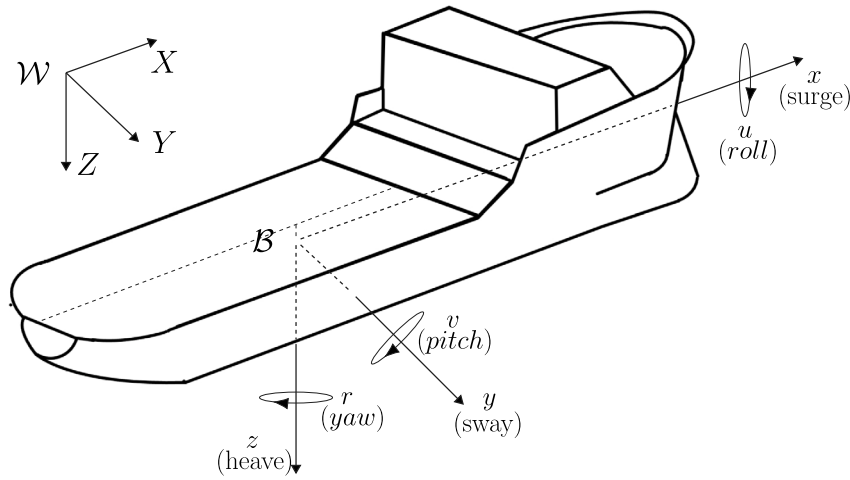
$C_{RB} \in R^{3 \times 3}$ and $C_A \in R^{3 \times 3}$ are the rigid body Coriolis and centrifugal components as well as added-mass derivatives corresponding to the velocity coupling and can be defined as

$$C_{RB}(v) = \begin{bmatrix} 0 & 0 & -m(x_G r + v) \\ 0 & 0 & mu \\ m(x_G r + v) & -mu & 0 \end{bmatrix}, \quad (6)$$

Table 1

A summary of selected DP controllers reported in the literature.

Reference	Controller(s)	Scope of study		
		Simulation	Experiments	Comparing controllers
Tannuri and Morishita (2006), Nguyen et al. (2007)	PID	Yes	No	No
Brodtkorb et al. (2018), Alfheim et al. (2018)	PID	Yes	Yes	No
Rabanal et al. (2016)	PID, SMC	Yes	Yes	Yes
Sotnikova and Veremey (2013)	MPC	Yes	No	No
Hou et al. (2022)	Lag-MPC, Lag-NMPC	Yes	No	Yes
Veksler et al. (2016), Du et al. (2016), Wang et al. (2012)	NMPC	Yes	No	No
Hvamb (2001)	NMPC	No	Yes	No
Jayasiri et al. (2017)	NMPC, PID	Yes	No	Yes
Alagili et al. (2022)	NMPC, GNMPC, PID	Yes	No	Yes

**Fig. 1.** The coordinate system of generic dynamic positioning vessel.

$$C_A(v) = \begin{bmatrix} 0 & 0 & Y_{\dot{v}}v \\ 0 & 0 & -X_{\dot{u}}u \\ -Y_{\dot{v}}v & X_{\dot{u}}u & 0 \end{bmatrix}. \quad (7)$$

$D(v) \in R^{3 \times 3}$ represents the energy dissipative terms (drag) due to relative motion between the vessel and surrounding fluid. The drag effects are nonlinear and can be divided into linear and nonlinear components as $D(v) = D_L + D_{NL}(v)$, where

$$D_L = \begin{bmatrix} -X_u & 0 & 0 \\ 0 & -Y_v & -Y_r \\ 0 & -N_v & -N_r \end{bmatrix}, \quad (8)$$

$$D_{NL}(v) = \begin{bmatrix} X_{|u|u}|u| & 0 & 0 \\ 0 & -Y_{|v|v}|v| - Y_{|r|v}|r| & -Y_{|v|r}|v| - Y_{|r|r}|r| \\ 0 & -N_{|v|v}|v| - N_{|r|v}|r| & -N_{|v|r}|v| - N_{|r|r}|r| \end{bmatrix}^T. \quad (9)$$

The forces applied to the vessel can be expressed as $\tau = \tau_c + \tau_w$, where τ_c is the forces from the thrusters, and τ_w is the force exerted on the vessel by the ocean waves. The constants, m , x_G , I_Z , $X_{\dot{u}}$, $Y_{\dot{v}}$, $Y_{\dot{r}}$, $N_{\dot{v}}$, $N_{\dot{r}}$, $X_{|u|u}$, $Y_{|v|v}$, $Y_{|r|v}$, $Y_{|v|r}$, $Y_{|r|r}$, $N_{|v|v}$, $N_{|r|v}$, $N_{|v|r}$, $N_{|r|r}$ are vessel-specific constants, and they are identified through system identification.

3. Green-NMPC theory

In this study we compare our energy efficient Green NMPC with other traditional controllers. A detailed formulation of the Green NMPC and simulation results are presented in Alagili et al. (2022). This

section presents a concise overview of the Green NMPC to enhance the readability of the manuscript.

The continuous time dynamics of the vessel described in the previous section can be converted to a discrete time dynamic system as

$$\chi_{k+1} = f(\chi_k, v_k), \quad (10)$$

where f is the nonlinear system dynamics with states, $\chi = [\eta^T, v^T]^T$, and inputs $v = \tau_c$. In practical applications, the states and the inputs have constraints and the linear or nonlinear constraints can be defined as

$$g(\chi_k, v_k) \leq 0. \quad (11)$$

The objective on NMPC is to determine the control actions v_k that minimize a cost function while satisfying the constraints given in (11). The cost function of the proposed GNMPC comprises of the economic cost function and the quadratic regularization term. The economic cost function $\varphi^{ec}(\chi_k, v_k)$, is defined as follows:

$$\varphi^{ec}(\chi_k, v_k) = L_x (F_{x,k} - F_{x,k-1})^2 + L_y (F_{y,k} - F_{y,k-1})^2 + L_\psi (T_{\psi,k} - T_{\psi,k-1})^2 \quad (12)$$

where, F_x , F_y , T_ψ are the thruster forces in surge and sway directions and the torque for yaw rotation, respectively, and $\tau_c = [F_x, F_y, T_\psi]^T$. L_x , L_y , L_ψ represent the weights associated with the control actions. When the cost function is not strongly convex, a quadratic regularization term is added to the cost function (Miller et al., 2010). The

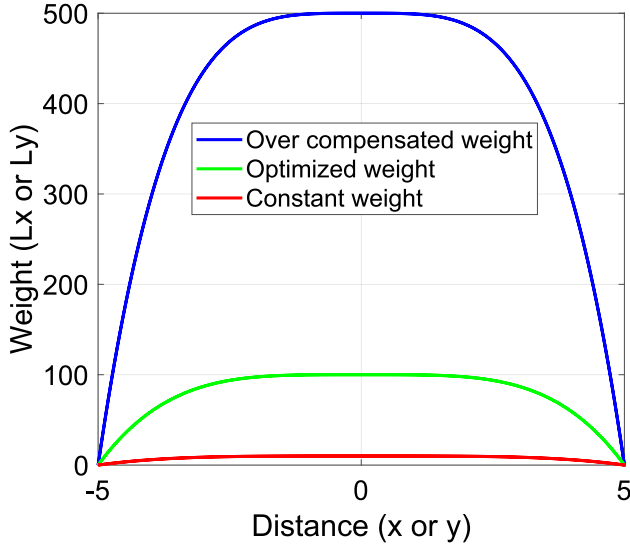


Fig. 2. Acceptable shape of weighting function for GNMPc.

regularization term has the following form:

$$\varphi^{rc}(\chi_k, v_k) = (x_k - x_r)^2 \pi_1 + (y_k - y_r)^2 \pi_2 + (\psi_k - \psi_r)^2 \pi_3, \quad (13)$$

where x_r, y_r, ψ_r are the reference position and heading, and π is the weight matrix. The total stage cost function can be expressed as

$$\begin{aligned} \varphi(\chi_k, v_k) &= \varphi^{ec}(\chi_k, v_k) + \varphi^{rc}(\chi_k, v_k) \\ &= L_x (F_{x,k} - F_{x,k-1})^2 + L_y (F_{y,k} - F_{y,k-1})^2 + L_\psi (T_{\psi,k} - T_{\psi,k-1})^2 \\ &\quad + (x_k - x_r)^2 \pi_1 + (y_k - y_r)^2 \pi_2 + (\psi_k - \psi_r)^2 \pi_3. \end{aligned} \quad (14)$$

The formulation of the NMPC problem can be expressed as follows:

$$\begin{aligned} \arg \min_{\chi_k, v_k} \sum_{j=k+1}^{k+N} \varphi(\chi_j, v_j) \\ \text{subjected to} \end{aligned} \quad (15)$$

$$\chi_{j+1} = f(\chi_j, v_j),$$

$$g(\chi_j, v_j) \leq 0, \quad \forall j \in [k, k+N].$$

Weights used in the objective function play a critical role in shaping the optimization objective. The weights $L = [L_x \ L_y \ L_\psi]$ governs the penalization of input variations, while $\pi = [\pi_1 \ \pi_2 \ \pi_3]$ determines the penalty for state errors. When a higher weight values are chosen for a specific component, it results in a greater penalty for changes of the corresponding component during optimization. This effectively steers the optimizer towards minimizing the associated error or variations in the control inputs. A traditional NMPC uses constant weight values and the values are tuned for the best performance. However, the proposed Green NMPC introduces variable weights in the cost function, and the variable weights are specified to satisfy two key performance requirements.

1: When the vessel is well within the safety limits, the main focus of the controller is to reduce energy consumption.

2: When vessel approaches the safety limit the focus of the controller shifts to maintaining the vessel at the set position.

When the vessel is well within the safety limits, the weights corresponding to the surge and sway thruster forces are adjusted to a high value. The higher weights force the optimizer to penalize variations in the thruster forces. Therefore, when the vessel deviates from the set point, the controller does not perform sudden thruster variations. As a result, the overall thruster demands are greatly reduced, and this

behavior allows the vessel to drift inside the safe operation zone instead of closely maintaining the set point.

When the vessel is approaching the safety limits, the weights corresponding to the surge and sway thruster forces are adjusted to a lower value, allowing drastic changes in the thruster values. This allows the controller to perform quick maneuvers and bring the vessel back to the desired set point.

The weight functions for (L_x, L_y) were set as continuously varying nonlinear functions of the respective position error to satisfy the aforementioned requirements. For instance, L_x is defined as a function of e_x satisfying the aforementioned conditions and penalizes the variations of thruster force F_x . Acceptable shape of the wave function is shown in Fig. 2. The weights can be selected to be over compensated (blue line of Fig. 2), where the controller focus more on maintaining the position, or be lenient (green line of Fig. 2), where the vessel is allowed to drift a longer distance. After much trial and error, we finally settled on the nonlinear function specified in Eq. (16) for the experiments.

$$L_x = 100 - \frac{e_x^4 (\log(|T_{th}|) - |e_x|)}{|T_{th}|}, \quad (16)$$

where, T_{th} is the position threshold, and e_x is the position error of the vessel along x axis. L_y is also defined similarly.

The constraints of the GNMPc expressed in (11) comprise of the upper and lower bounds of the states and inputs. The constraints can be expressed as

$$g(\chi_k, v_k) = \begin{bmatrix} \chi_k - \chi_{max} \\ -\chi_k + \chi_{min} \\ v_k - v_{max} \\ -v_k + v_{min} \end{bmatrix} \quad (17)$$

4. Methodology and experimental setup

This section provides a comprehensive overview of the experimental setup employed in our study. The overall configuration of the experimental setup is shown in Fig. 3. Additionally, we present the system identification process, where we aim to accurately characterize the dynamics and behavior of the ship. Furthermore, we detail the implementation of the wave filter utilized in our experiments. The wave filter is a crucial component that mitigates the response to high-frequency wave action, that is outside the vessel response capability, or efficient bandwidth of control. Finally, we outline the test cases that were executed to evaluate and compare the three controllers. These test cases were carefully designed to evaluate the performance and robustness of the system under different conditions and scenarios.

4.1. Experimental setup

The experiments were carried out in the Offshore Engineering Basin (OEB) at the National Research Council (NRC) Ocean, Coastal, and River Engineering Research Center in St. John's, Canada. The OEB facility is one of the world's most advanced indoor model ocean facilities. The basin, which measures 75 m by 32 m by 4 m, can simulate extreme model sea-state conditions that happen only once per 10,000 years (scale dependent). The OEB is equipped with 168 individually controlled and vertically adjustable wave-maker modules in a fixed "L" configuration. Each segment is 2 m high and 0.5 m wide and are grouped together in fours to form a module. The wave-maker system can generate unidirectional or multi-directional waves up to 1 m tall. Passive wave absorbers are fitted around the other two sides of the tank. The basin can also produce wind to replicate actual sea conditions. The basin is capable of testing models at a reasonably large scale and evaluates concepts in a controlled environment to get high-quality, realistic results.

The experiments of the DP controllers were carried out on a scaled model of a Magne Viking supply vessel (Fig. 4). The model ship is a

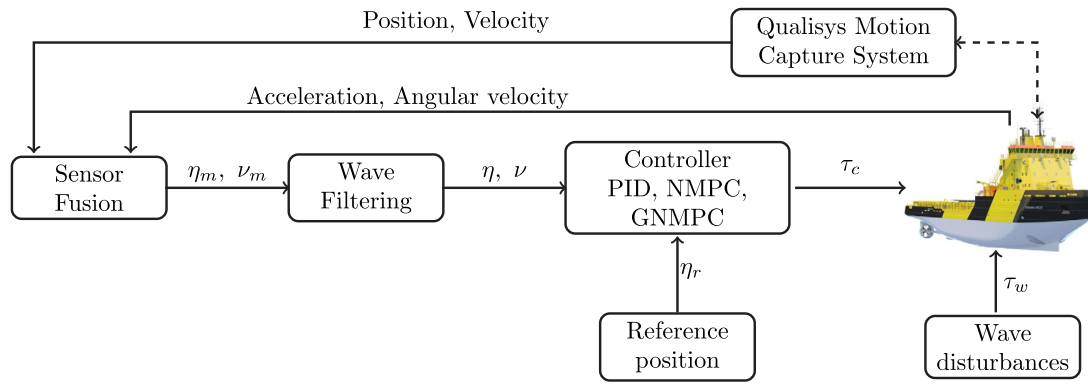


Fig. 3. Flowchart of the experiments.

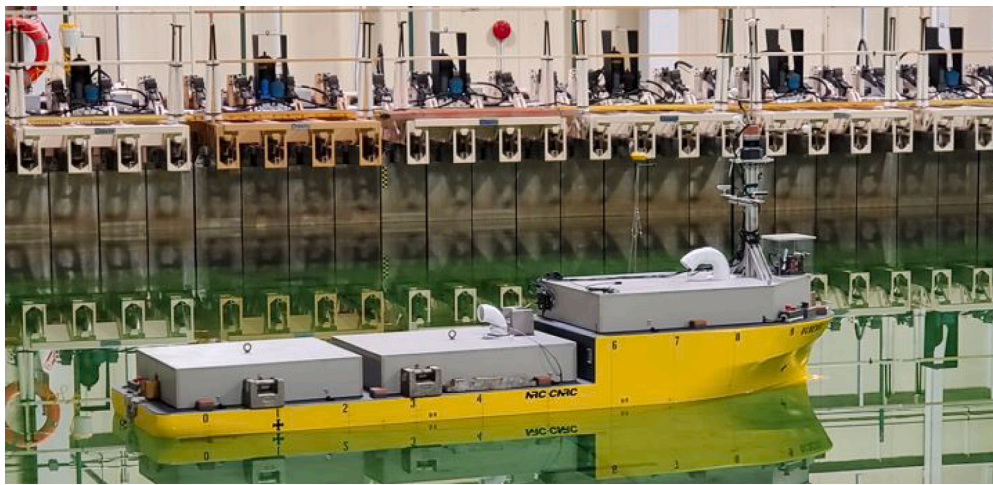


Fig. 4. The Magne Viking model vessel.

1:19.5 scale model of the actual vessel and has the following dimensions: mass (m) = 1229 kg, length (L), 4.44 m, and width (B) = 1.16 m. The vessel is equipped with two main propellers, one bow thruster, and one stern thruster for propulsion.

A computer onboard the model vessel controls the internal hardware including the propulsion system, collect sensor data from onboard sensors and communicate with the main control computer through the Data Acquisition System (DAS) network. The OEB is equipped with a Qualisys motion capture system that measures the Earth-fixed position orientation and speed of the vessel. Active markers are placed on the model to allow the motion tracking using the cameras mounted around the basin. The Qualisys motion capture system is capable of providing position feedback with 1 mm accuracy. However, in practice there can be dropouts due to the sheer size of the OEB tank. To minimize the effects of dropouts, an EKF is implemented to fuse inertial measurements from the vessel with the motion capture feedback.

The Magne Viking model is retrofitted with Crossbow VG700CB-200 inertial measurement unit (IMU). The IMU measures the accelerations and angular rates of the vessel, and these measurements are used in an EKF based attitude heading reference system (Johansen and Brekke, 2016). The EKF predicts the position and orientation at 50 Hz using the measurements from the IMU, and then do the correction based on the absolute position and orientation measurements from the motion capture system. The AHRS allows the controller to have an accurate, uninterrupted feedback even during a dropout of motion capture feedback.

The NMPC and GNMPC controllers run on a separate computer, which is connected to the main control computer via the OPC server. The communication setup between the model, motion capture system, and the main and secondary control computers is shown in Fig. 5.

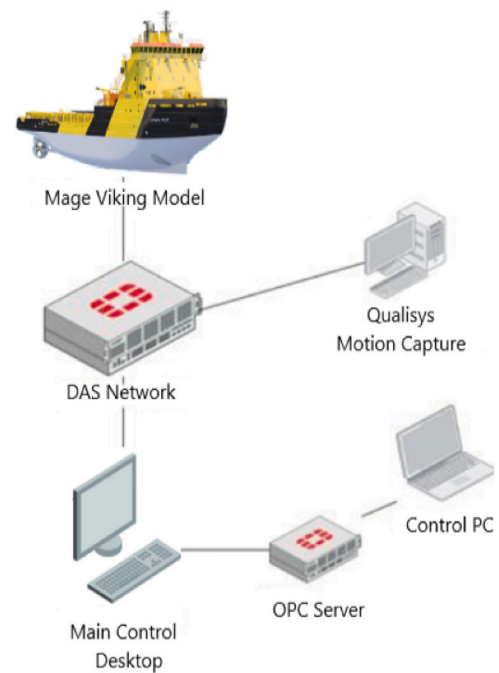


Fig. 5. Communication network.

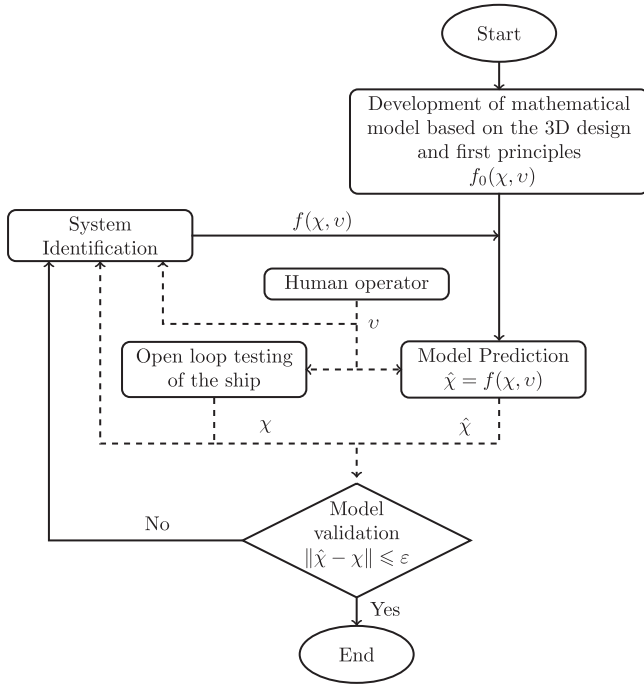


Fig. 6. Workflow of system identification.

4.2. System parameter identification

The performance of an MPC depends on the quality and accuracy of the vessel's model. Hence, an accurate mathematical representation of the vessel's dynamics is essential for successful MPC implementation. In the case of the experimental setup involving the scaled model of the Magne Viking supply vessel, the physical parameters, such as mass, length, etc. were identified through a set of comprehensive measurements. The initial hydrodynamic parameters were calculated using the 3D model of the model vessel. Over time, several modifications were made, and several sensors were added to the initial design to improve the capabilities of the model. During experiments it became apparent that the initial parameters no longer adequately reflected the true dynamics of the modified ship. Therefore the new model parameters had to be identified.

Multiple approaches exist for parameter identification in models. A common method involves separating transient and steady-state elements and using linear regression to estimate parameter values. In a study by Eriksen and Breivik (2017), a non-first-principles model was identified for a high-speed autonomous surface vehicle's motion. The parameter values were determined through weighted linear least squares regression with a regularization term to discourage large parameter values. The model's accuracy was verified by comparing simulated vessel response with experimental data and was subsequently employed in a controller with feed-forward terms. In another study by Fossen et al. (1996), an offline parallel extended Kalman filter (EKF) algorithm was utilized to estimate parameters for a nonlinear dynamic positioned ship model. A decoupled identification scheme involved three different ship maneuvers, with parameters from one scheme serving as input for the next until all parameters were identified. The approach's effectiveness was verified by implementing and testing it on a supply vessel, with the results compared against experimental data. In our experiments, we used the optimization-based system identification technique that was developed in Pedersen (2019).

We piloted the vessel at various speeds and in various trajectories to collect data. When sufficient motion data are available we conducted

the identification and validation workflow shown in Fig. 6. The optimization technique calculates the system parameters by minimizing a weighted sum of square errors. The objective function is defined as

$$L(x, \hat{\chi}) = \sum_{k=t_0}^{t_0+T_s} (x_k - \hat{\chi}_k)^T W (x_k - \hat{\chi}_k) \quad (18)$$

$$\hat{\chi}_k = f(x_{k-1}, v_{k-1}, \Theta),$$

where f is the ship dynamics given in (3), and Θ is the vector of physical and hydrodynamic parameters to be identified.

$$\Theta = [I_z, X_{\dot{u}}, Y_{\dot{v}}, Y_r, N_{\dot{v}}, N_r, X_u, Y_v, Y_r, N_v, N_r, X_{|u|u}, Y_{|v|v}, N_{|r|r}] \quad (19)$$

x is the measured state vector of the ship. $\hat{\chi}$ is the calculated states based on the system dynamics given in (1) and (3). The weight matrix W is defined $W = \text{diag}(W_1, W_2, W_3, W_4, W_5, W_6)$, where $W_i > 0$. Proper initialization is crucial when performing optimization, and the parameters identified using the measurement and the 3D model are used as the initial values for the optimization. Calculated parameters are shown in Table 2.

4.3. Wave filter setup

The motion of a ship under the influence of waves is generally modeled as the superposition of low-frequency (LF) and wave-frequency (WF) motion components. The LF motions, i.e., drift, result from second-order wave drift forces and control thrust forces. On the other hand, the WF motions are predominantly caused by first-order wave motions, leading to the vessel's oscillatory movements. Controlling the vessel based on the oscillatory position feedback can lead to excessive control actions and poor DP performance.

There has been extensive research on the WF for DP systems. In the study by Sørensen et al. WF filtering was employed by utilizing Kalman filter theory and assuming linearization of the ship's kinematic equations around predefined constant yaw angles (Sørensen et al., 1996). This approach was necessary for the application of linear Kalman filter theory and gain scheduling techniques. In Fossen and Strand (1999), a nonlinear observer incorporating wave filtering capabilities and bias estimation was developed based on the principle of passivity. Furthermore, Torsetnes et al. (2004) introduced gain scheduled wave filtering as an additional technique. In our experiments, we utilized the wave filtering approach proposed in Fossen and Strand (1999) for effective filtering of wave disturbances.

In Fossen (2002), Fossen derives a linear state space model for the first-order wave response. The response model in surge, sway, and heading can be expressed as

$$\dot{\xi} = A_w \xi + E_w w_2 \quad (20)$$

$$\eta_w = C_w \xi, \quad (21)$$

where $\xi \in R^6$ is the state vector, and $w_2 \in R^3$ is a zero-mean Gaussian white noise. Matrices $A_w \in R^{6 \times 6}$, $E_w \in R^{6 \times 3}$, and $C_w \in R^{3 \times 6}$ are constant matrices defined as

$$A_w = \begin{bmatrix} 0_{3 \times 3} & I_{3 \times 3} \\ -\Omega_{2 \times 3} & -A_{3 \times 3} \end{bmatrix}, \quad E_w = \begin{bmatrix} 0_{3 \times 3} \\ I_{3 \times 3} \end{bmatrix}, \quad C_w = [0_{3 \times 3} \quad I_{3 \times 3}],$$

with

$$\Omega = \text{diag}(\omega_1, \omega_2, \omega_3) \quad \Lambda = \text{diag}(2\omega_1\zeta_1, 2\omega_2\zeta_2, 2\omega_3\zeta_3)$$

where $\omega = [\omega_1, \omega_2, \omega_3]$ is the dominant wave frequency, and $\zeta = [\zeta_1, \zeta_2, \zeta_3]$ is the relative damping coefficients.

η_w is the WF motion of the ship due to the first-order waves. Effects of the second-order mean and slowly varying wave loads are modeled as a random walk process (Wiener process) and can be expressed as

$$\dot{b} = w_3 \quad (22)$$

where $w_3 \in R^3$ is a vector of zero-mean Gaussian white noise.

Table 2
Identified parameter values of Magne Viking model.

Physical Parameter	Value	Identified parameter	Value	Identified parameter	Value
Length	4.44 (m)	I_Z	1577.65 (kgm ²)	X_{θ}	158.23
Beam	1.16 (m)	Y_{ϕ}	1087.3	Y_r	~0
m	1358.5 (kg)	N_{ϕ}	~0	N_r	1559.92
x_G	0.18 (m)	X_u	41.788	Y_{ψ}	336.06
		Y_r	~0	N_{ψ}	~0
		N_r	26	$X_{ u u}$	194
		$Y_{ \psi }$	~0	$N_{ r }$	3913.5

The bias $b \in \mathbb{R}^3$ is incorporated into the ship's dynamics in (1) as a bias force, and the modified dynamics can be expressed as

$$M_{RB}\dot{v} + M_A\dot{v} + C_{RB}(v)v + C_A(v)v + D(v)v = \tau_c + J(\psi)^T b + w_1 \quad (23)$$

where $w_1 \in \mathbb{R}^3$ is a vector of zero-mean Gaussian white noise.

In this study, we implemented a UKF-based wave filter to filter out the WF motions due to waves. UKF performs the propagation of the uncertainties of the Gaussian Random Variable (GRV) through a deterministic sampling method (unscented transform). Using Eqs. (3), (23), (20), and (22), the process model used for the UKF can be expressed as

$$\dot{\eta} = J(\psi)v \quad (24)$$

$$\dot{v} = (M_{RB} + M_A)^{-1} (-C_{RB}(v)v - C_A(v)v - D(v)v + \tau_c + J(\psi)^T b + w_1) \quad (25)$$

$$\dot{\xi} = A_w \xi + E_w w_2 \quad (26)$$

$$\dot{b} = w_3 \quad (27)$$

Feedback for the experiment was obtained through the Qualisys motion capture system, which provided the ship's position and heading. The measured position and heading can be modeled using the linear superposition of the WF motion component and the LF motion component. Hence the position and heading measurement can be modeled as

$$y = \eta + \eta_w + w_4 \quad (28)$$

where $w_4 \in \mathbb{R}^3$ is the measurement noise vector.

Jayasiri et al. (2017), Julier and Uhlmann (1997), Deng et al. (2019). Mathematical formulation and implementation of UKF are well documented in the literature and the UKF pseudo code is shown in Algorithm 1. Detailed implementation of UKF can be found in Julier and Uhlmann (1997), Deng et al. (2019).

Algorithm 1: UKF-Based Wave Filter

- 1 Initialize the states (Ξ) and their covariance (P_{Ξ}),
 $\Xi = [\eta^T, v^T, \xi^T, b^T]^T$;
 - 2 **for** $k \in (1, \dots, \infty)$ **do**
 - 3 Calculate sigma points for states (Ξ) and measurements (y);
 - 4 Propagate the sigma points through system model
 (24)–(27);
 - 5 Compute the predicted mean and covariance Ξ_{k^-}, P_{Ξ,k^-} ;
 - 6 Propagate the measurement sigma points through
 measurement model (28);
 - 7 Read pose and velocities of the vessel;
 - 8 Calculate the Kalman gain;
 - 9 Compute the updated sates and covariance Ξ_{k^+}, P_{Ξ,k^+} ;
 - 10 **end**
-

The wave filter was tuned for each type of wave. This involves adjusting the tuning matrix A_w in (20) based on the dominant frequency of the wave and appropriate damping coefficients. The initial guess of the dominant frequency was determined by analyzing the wave

Table 3
Tuning parameters of wave filter.

Wave type ^a	Dominant frequency	Damping coefficient
White Noise Wave	[2.1, 2.1, 2.1]	[0.02, 0.02, 0.02]
Irregular Wave	[2.3, 2.3, 2.3]	[0.01, 0.01, 0.01]
Regular Wave	[2.7, 2.7, 2.7]	[0.02, 0.02, 0.02]

^a See Table 4 for the definitions of waves.

spectrum, and then fine-tuned through a process of trial and error. The values used for ω and ζ are shown in Table 3

Fig. 7 illustrates the measured position and heading of the ship influenced by a regular wave and the LF motion of the ship after filtering the WF motion. Fig. 7 demonstrates that the wave filter based on UKF successfully estimates the WF motion components from the feedback and produces LF motion feedback for the controller.

4.4. Controller implementation

The proposed GNMPC is optimization based control algorithm, which calculates the optimum control actions by solving the optimization problem defined in (15) at each time step. Optimization based algorithms demand significant computational resources and may result in longer execution times posing challenges for real-time implementation. The optimal control problem was formulated using direct multiple shooting (DMS) approach. We opted for the DMS approach due its robustness to model uncertainty and better convergence (Diehl et al., 2006). However, the DMS approach has more optimizing variables which lead to increased computational complexity.

In this study we used the CasAdi framework to implement the NMPC and Green NMPC controller (Andersson et al., 2019). CasAdi is an open-source software framework that provides a powerful set of tools for modeling and solving optimization problems. CasAdi supports a variety of programming languages, including Python, MATLAB, and C++, making it versatile. As the solver for the optimization problem we selected built-in interior point optimizer (IPOPT). IPOPT algorithm is computationally efficient and can handle large-scale optimization problem generated using DMS approach.

The NMPC and GNMPC controllers are implemented using MATLAB in a laptop equipped with AMD Ryzen 5 5600H and 16 GB of RAM. Number of samples in the prediction horizon is a key factor determining the execution time of the controller. Since the vessel has slow dynamics, a controller with shorter prediction horizon does not yield the best performance. Controller with a longer prediction horizon performs better but with a longer execution time. After much trial and error, we decided a prediction horizon of 16 s, 80 prediction horizon samples at 5 Hz. The selected controller rate and number of samples provided a better compromise between the performance and computation time.

The controller communicates with the main control computer through the OPC server at 5 Hz. In each iteration, the controller request the pose and velocity feedback of the vessel, and then the control actions are forwarded to vessel. The state and input limits used in (17)

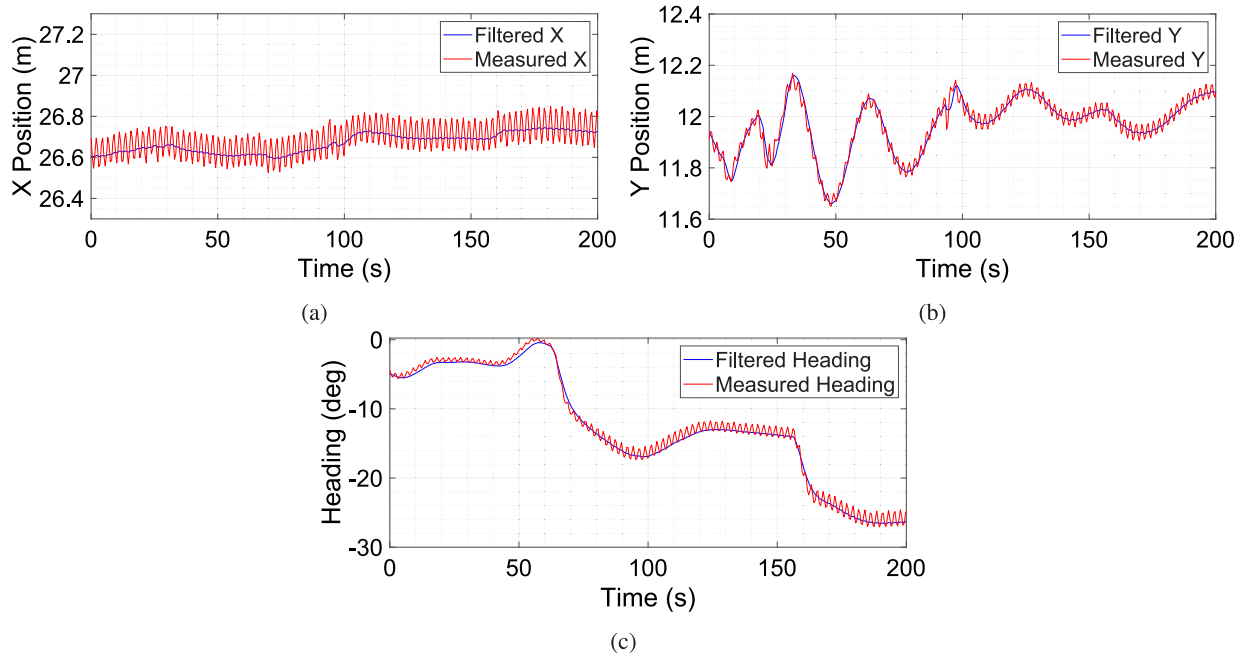


Fig. 7. Position and heading of the ship under the influence of regular waves.

Table 4
Definition of waves.

ID	Significant wave height, H_s [m]	Peak wave frequency ω_p [rad/s]	Wave type
1	0.178	2.3	Regular
2	0.178	Range	White noise
3	0.1	1.26711	Irregular, Short crest

are selected based on the experimental setup. The limits used in the experiment are as follows

$$\begin{aligned}
 \chi_{max} &= [0 \text{ (m)}, 0 \text{ (m)}, 2\pi \text{ (rad)}, 0.3 \text{ (ms}^{-1}\text{)}, 0.3 \text{ (ms}^{-1}\text{)}, -0.3 \text{ (rads}^{-1}\text{)}] \\
 \chi_{min} &= [-75 \text{ (m)}, -32 \text{ (m)}, -2\pi \text{ (rad)}, -0.3 \text{ (ms}^{-1}\text{)}, \\
 &\quad -0.3 \text{ (ms}^{-1}\text{)}, -0.3 \text{ (rads}^{-1}\text{)}] \\
 v_{max} &= [35\text{N}, 45\text{N}, 65\text{N}] \\
 v_{min} &= [-35\text{N}, -45\text{N}, -65\text{N}]
 \end{aligned}
 \tag{29}$$

4.5. Test cases

A key contribution of this paper is conducting experiments under different wave conditions in a controlled environment. Wavemakers in OEB can generate various types of waves. Based on the height and period, the waves can be divided into sea states. In this study we chose three different wave conditions along with no wave condition (NW) to compare controller performances. Waves are characterized by the peak wave frequency and the significant wave height. The characteristics of the waves used in the experiments are listed in Table 4.

The regular waves (RW) are waves with a single frequency and periodic wave height, period, and wavelength. The irregular waves (IRW) are a superposition of several regular waves, which have a significant wave height, and a dominant frequency. The white noise waves (WNW) has a wide frequency range with a flat power spectrum (Cavaleri et al., 2007). The WNW used in this study has an incident angle of 20 degrees, whereas the other two waves, have zero incident angle.

In this study we carried out three different tests, 1: DP at head seas (HS), 2: DP at oblique angles (OA), 3: DP with large setpoint changes

Table 5
Summary of experiments.

Wave type	PID	NMPC	GNMPC
No Wave	HS, OA, LSP	HS, OA, LSP	HS, OA
White Noise Wave	HS, OA, LSP	HS, OA, LSP	HS, OA
Irregular Wave	HS, OA, LSP	HS, OA, LSP	HS, OA
Regular Wave	HS, OA, LSP	HS, OA, LSP	HS, OA

(LSP). These tests were carried out under different wave conditions, and with each controller. During each experiment, the vessel was initially maneuvered to the initial set point in calm waters, and once the vessel was in position the waves were introduced. Through out this transition, each controller was actively controlling the vessel. The experimental data was collected once the waves reached a steady state condition. We conducted a total of 32 experiments and a summary of the experiments is shown in Table 5.

5. Experimental results

This section presents the comprehensive results obtained from the DP tests conducted under different wave conditions. Three tests, HS, OA, and LSP, were carried out to assess and compare the performance of the three controllers. The experiments aimed to evaluate the effectiveness of the dynamic positioning system in different challenging situations. Due to space limitations, this paper will present the plots showing the position holding, and spectral density of the thrusters of the controllers only for the regular wave (RW) conditions. All other results are reported for no wave (NW), white noise wave (WNW), irregular wave (IRW) and regular wave (RW) conditions.

5.1. DP head seas

The main task of the DP head seas experiment is to maintain the vessel at a given position with zero heading amidst disturbances. In most of the practical DP applications, the heading of the ship will be adjusted to match the wave direction.

Fig. 8 shows the position and heading accuracy of the three controllers under the four sea conditions. The bars in the plot represent

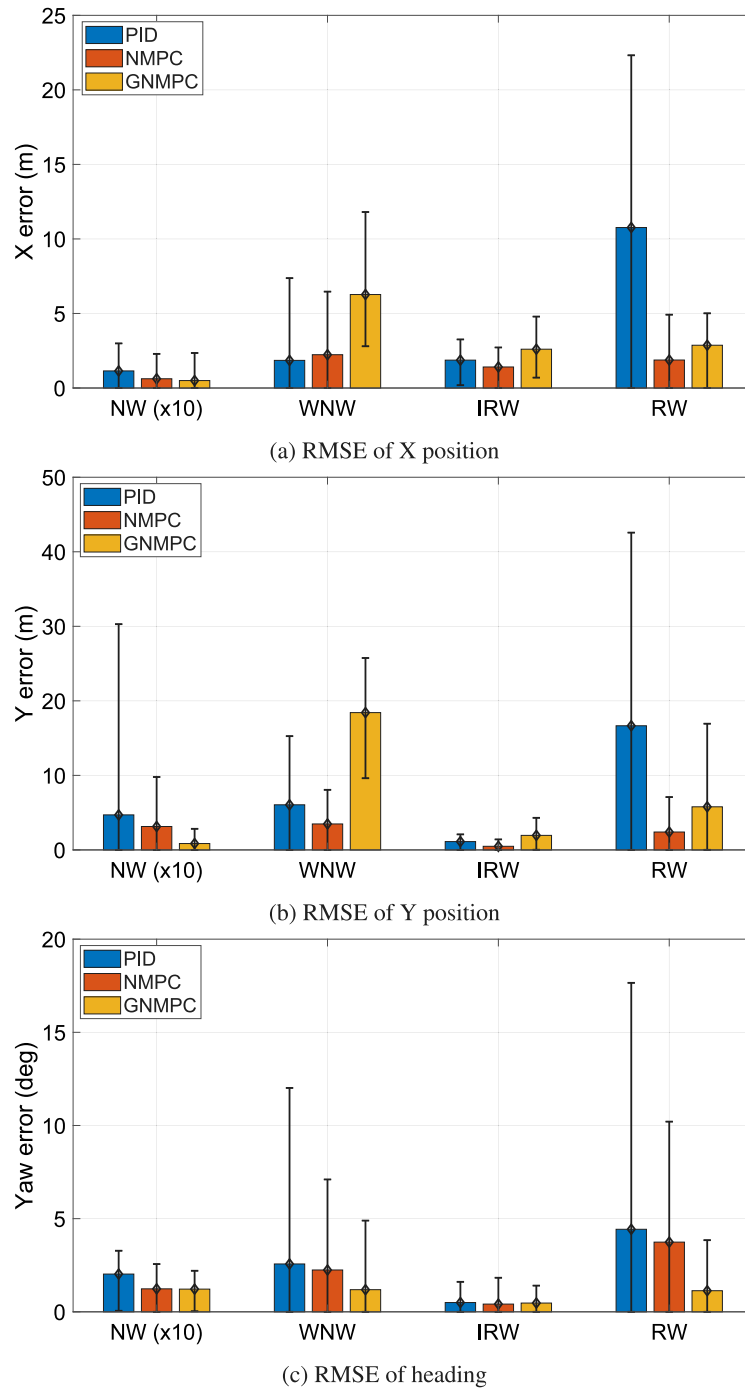


Fig. 8. Position and heading accuracy of HS tests under different wave conditions.

the root mean square error (RMSE) values for each test, with the height of each bar corresponding to the magnitude of the mean error. The error bars on each bar indicate the 95% confidence interval of the root square errors. Under the NW conditions, all controllers' errors are extremely small. The maximum position error is around 3% of the total ship length. The coupling effect of the four propellers can cause motion in the ship. The PID tries to minimize the error in the set point, and therefore, the PID has more actuator movements. NMPC considers the dynamics of the ship and calculates the optimum control action. Therefore, the corrections applied by the controller are less aggressive than the PID, and the errors are less. Since the vessel is within the safety boundary, the GNMPC does not make any corrections. Therefore, disturbances due to the coupling effects are less and the accuracy is

the highest. Under the WNW conditions, the NMPC provides the best performance in terms of accuracy. The x position RMSE of the PID controller is lower compared to the NMPC, but when closely observing, we can see the maximum error of the PID controller is higher than the maximum error of the NMPC. The error of the GNMPC is larger compared to both PID and the NMPC. However, we can see that the GNMPC errors did not exceed the safety limit. Since the white noise reached the ship at an oblique angle, the wave pushed the ship to one side of the set point. We can see the minimum RMSE has a positive value, which shows a drift of the ship to one side of the set point. Under the IRW conditions, the vessel movement is small. We can see a higher accuracy in the NMPC compared to the PID. GNMPC error is larger compared to both NMPC and PID. In order to maintain the ship within

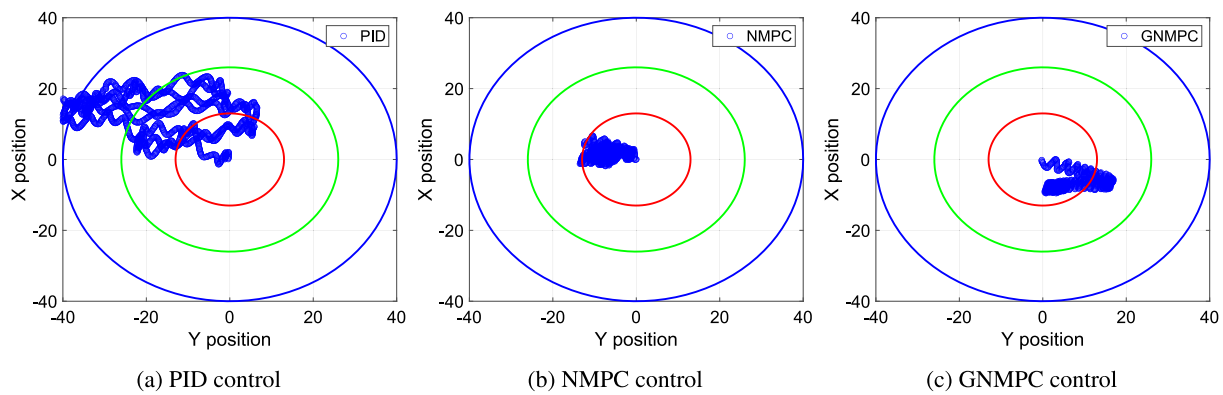


Fig. 9. Comparing the position holding performance of PID, NMPC, and GNMPC controller under regular wave.

the safety limit and has reduced thruster usage, the GNMPC allows the vessel to drift slightly. The regular wave is the most challenging wave for the vessel. We can clearly see a significant improvement in the accuracy of NMPC compared to the PID controller. Following a similar trend, the GNMPC position accuracy is lower compared to NMPC. When comparing the heading accuracies, the GNMPC has the highest accuracy compared to the PID and NMPC. Since dynamic weights are not assigned for the heading control, the GNMPC performs similarly to a NMPC controller for the heading correction. Since the thruster movements from the GNMPC controller are less compared to the NMPC, the cross coupling effects on the ship are minimized in the GNMPC controller. This results in a higher accuracy in the heading angle.

Fig. 9 shows the vessel's XY position for PID, MPC, and GNMPC controllers under regular wave case. Results indicate that the vessel locations were within the safe range in every case. Compared to the NMPC control, the PID has wider spread movements about the setpoint. Moreover, there is more vessel movement for Green-NMPC, as the point reference monitoring is relaxed to area tracking within the safety limitations. It is evident that the Green-NMPC's weight function is able to maintain a trade-off between maintaining position and limiting thruster motions.

Fig. 10(a) shows the energy consumption of the three controllers under each wave condition. We can observe that the GNMPC controller has the lowest power consumption compared to the PID and NMPC. The PID controller has the highest power consumption.

The primary reason for preferring less variation in ship thrusters is to ensure safe and stable ship operations. The thrusters control the ship's movement and maintain its position, especially in dynamic positioning operations. If the thrusters' output varies too much at quick succession, it can lead to unstable ship movement. Moreover, excessive variation in thruster output can also cause unnecessary wear and tear on the thrusters and other ship components, leading to increased maintenance costs and downtime. Fig. 10(b), Fig. 10(c), and Fig. 10(d) show the spectrum of the forces on the x,y, and torque rotational axes under RW condition. It is clearly visible that the GNMPC has more low frequency movements compared to the rest of the controllers. This means that the GNMPC reduces high frequency variations in thrusters which can result in less wear and tear.

5.2. DP oblique angles

The DP oblique angles test is an additional dynamic positioning (DP) test used to confirm that a vessel can maintain its position at various angles. The vessel is then kept in the same X-Y orientation while rotating about its axis at 30, and 45 degrees. Fig. 11. shows the position and heading accuracy of the three controller under different sea conditions. The errors made in these tests are minimal in the no wave condition since there is no external disturbances. The ship may move as a result of the four propellers coupling effect. The PID

makes an effort to reduce setpoint errors. PID has more actuations as a result, which reduced its precision. The actuator actions by the other controllers are smaller than those made by PID since NMPC considers the ship's dynamics. Given the small position error, the GNMPC applies the least correction, resulting in the highest accuracy in no wave conditions. The RMSE of the PID controller at the white noise wave case in the X, and Y error position is marginally higher than the RMSE of the NMPC. A closer look at the results also show that the maximum inaccuracy in the PID is higher. Also it is observed that the NMPC performs better than the PID controller in X, and Y and heading error minimization. NMPC, and PID almost always have smaller errors than the GNMPC. However, the GNMPC position errors were within the acceptable safety limit. The white noise wave pushed the ship to one side of the setpoint due to the oblique angle. We can observe that the minimal root square error is positive, indicating that the ship is drifting to one side. Ship movement under irregular waves is small. When compared to the PID, the NMPC has a higher accuracy. The GNMPC error is larger than NMPC and PID errors. Regular waves are the most difficult waves to manage, the precision of the NMPC controller is significantly better than the PID controller in this situation. The GNMPC position accuracy is lower than NMPC, continuing a similar pattern. The vessel's trajectory on the XY plane under regular wave case is shown in Fig. 12. However, there is more vessel movement with GNMPC as area tracking is allowed instead of point reference monitoring within the bounds of safety. The GNMPC's weight function is able to maintain a trade-off between maintaining position and limiting thruster motions. To evaluate the control action's efficacy, the control signals' variance and power are analyzed. According to the results, GNMPC has the lowest overall power consumption as shown in Fig. 13(a). GNMPC control actions have lower gain in the mid and high frequency area, as seen in (Figs. 13(b), 13(c), 13(d)). This indicates that there will be less high-frequency movement in the thrusters which will help to keep the wear and tear of the thrusters to minimal.

5.3. Large position setpoint changes

Though the objective of DP is not to track trajectories, it is occasionally required to make small position changes during DP operation. This test is done to evaluate the controllers' ability to make small adjustments in position and angles. The controllers were tested for their ability to navigate to the four corners of a rectangular area under irregular wave conditions. Fig. 14 shows the trajectory tracked by the vessel under the PID and the NMPC. Note that GNMPC is not tested for trajectory tracking since its objective function is not suitable for position tracking. Depending on the state of the irregular waves, in the PID controller case, the ship departs from point (-33,15) and stops along the way at points (-28,15), (-28,10), (-33,10), and (-28,15) as illustrated in Fig. 14. In the NMPC case, the ship moves from the point (-27,14) to stops (-23,14), (-23,10), (-27,10), and

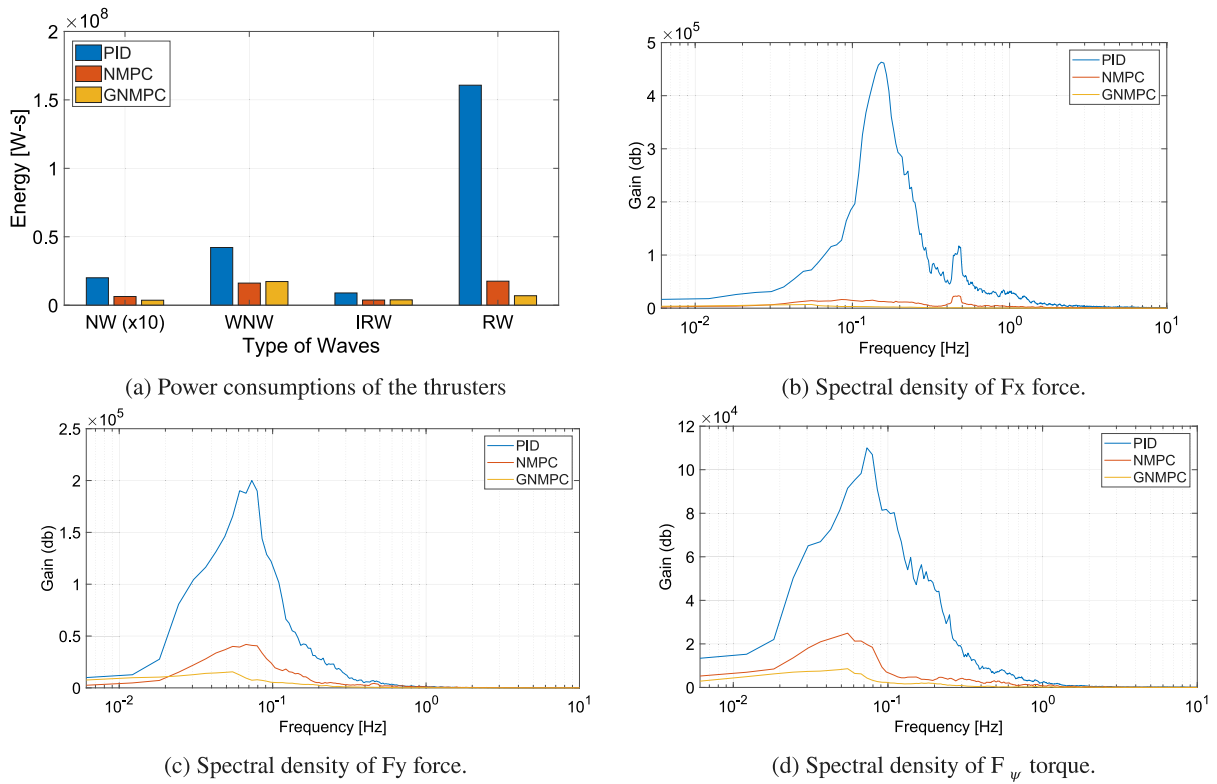


Fig. 10. Comparison of energy consumption of the HS test under different wave conditions and power spectrum of the thrusters under RW conditions.

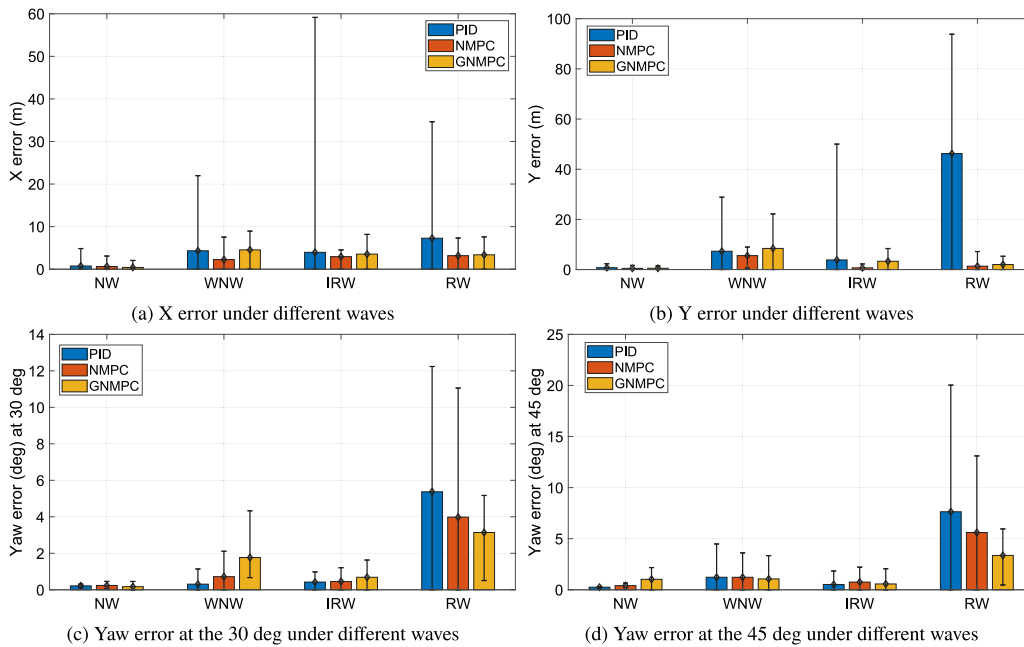


Fig. 11. Position and heading accuracy in DP angle setpoint change test under different wave conditions.

(-23,14). Furthermore, the Fig. 14. shows the NMPC performance is more stable and closer to meeting the trajectory reference than PID. Fig. 15(a) shows the energy usage of the two controllers for different wave situation. For all wave conditions the NMPC uses less energy than the PID control.

(Figs. 15(b), 15(c), 15(d)). shows that NMPC control actions have reduced gain in the high-frequency region indicating less high-frequency thruster movement.

6. Conclusion and final remarks

This study reports an experimental implementation of NMPC and an energy efficient GNMPC controller. This is one of the very few experiments where the NMPCs were tested in a controlled environment with varying wave conditions, and to the best of our knowledge, this is the first experimental implementation of the GNMPC. The extensive experiment tests provided many valuable insights which will be useful during the implementation of model based controllers on DP systems.

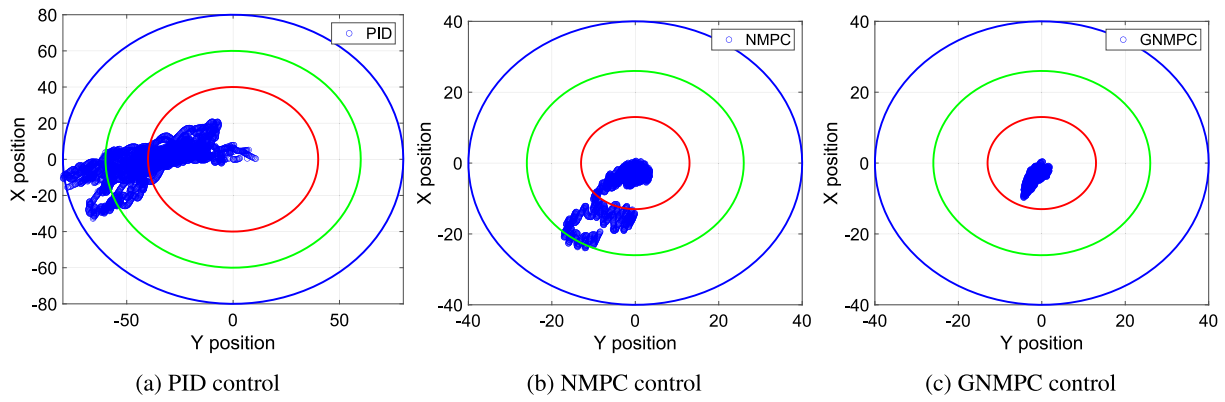


Fig. 12. Comparing the position holding performance of PID, NMPC, and GNMPC controllers under regular wave.

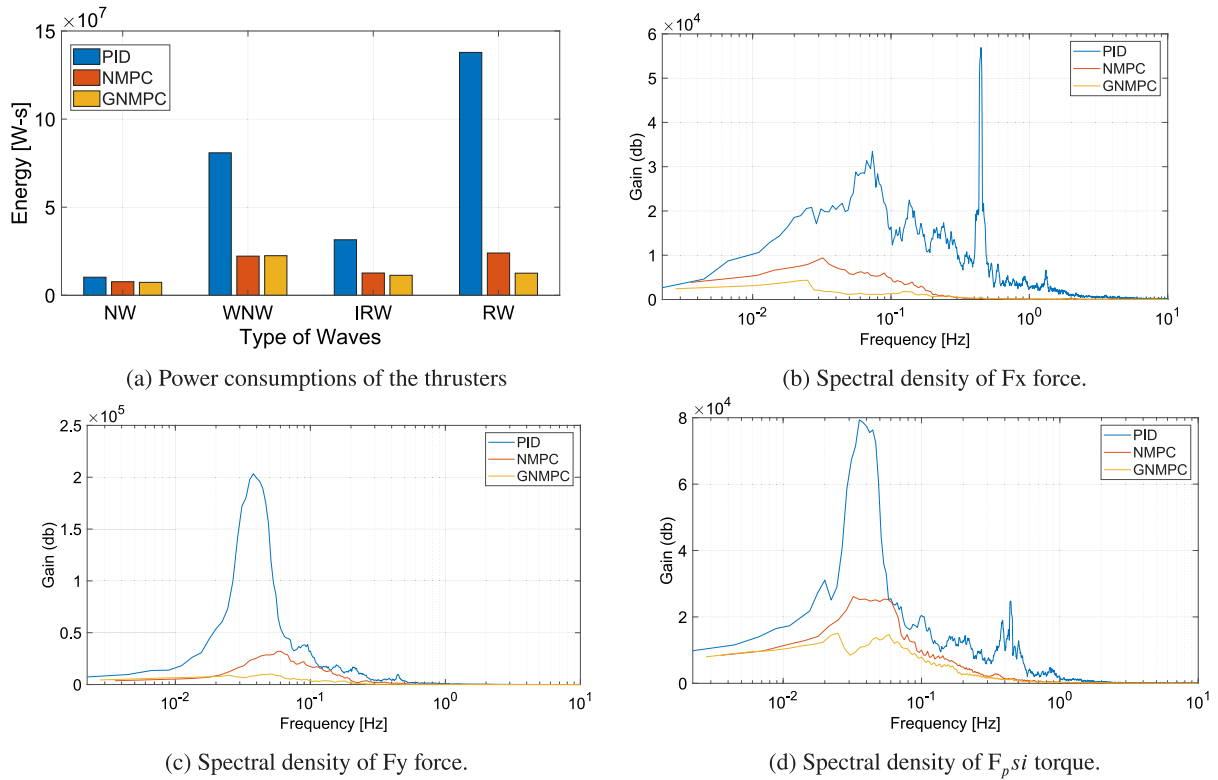


Fig. 13. (a) Power consumptions of the thrusters for the DP angle setpoint change test under different waves; and (b), (c), (d) power spectral of the thrusters in regular wave conditions.

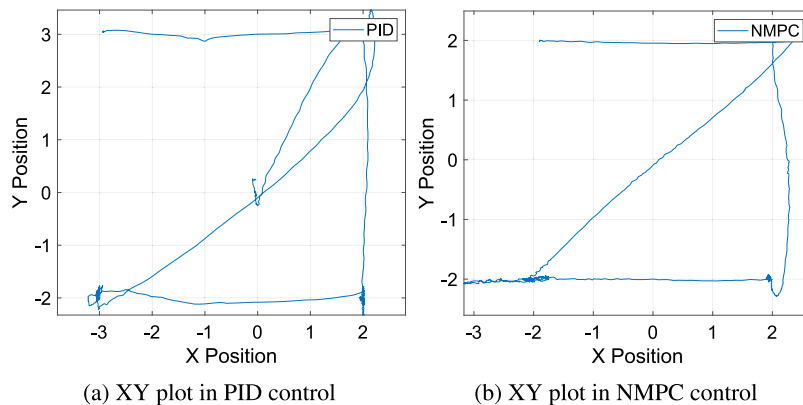


Fig. 14. Setpoint tracking using PID, and NMPC controllers: ship X,Y.

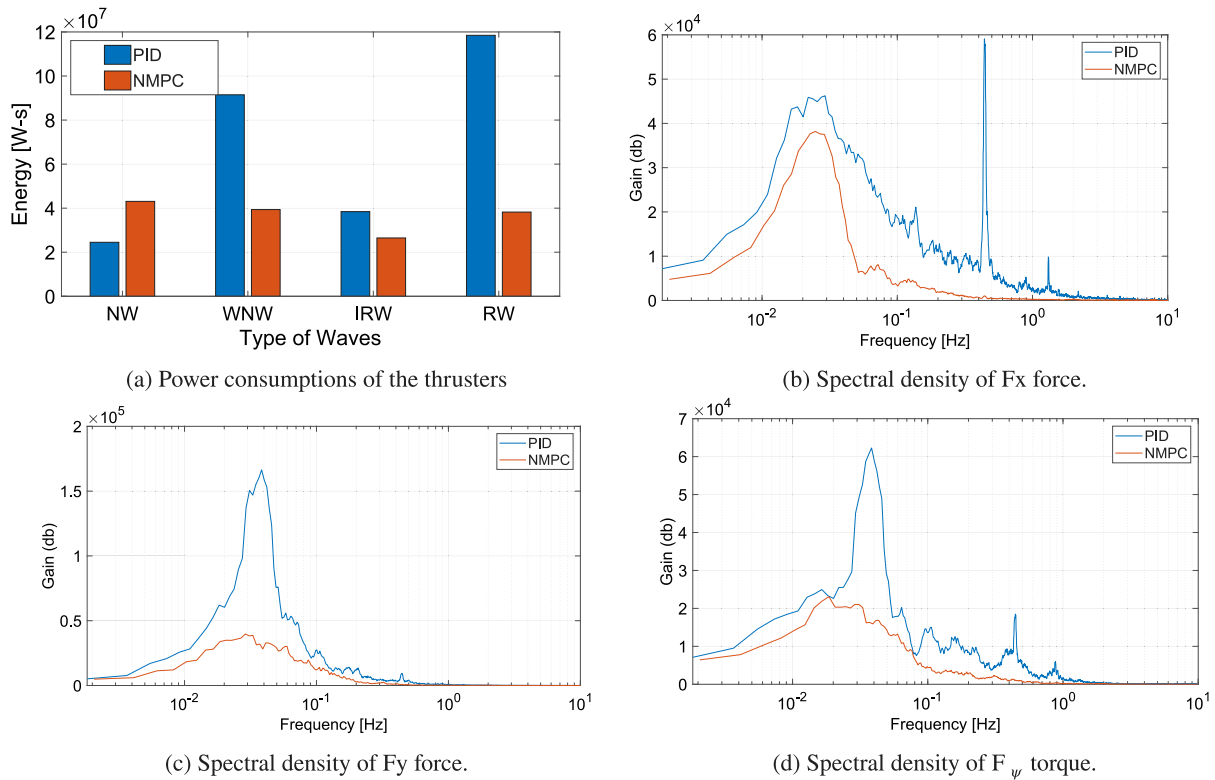


Fig. 15. Power consumptions of the thrusters for the large setpoint changes test under different waves and Power spectral of the thrusters in regular wave conditions.

The experimental results on the station keeping tests showed that on average, the GNMPC is the most energy efficient controller for the application. The GNMPC minimizes the thruster movement by implementing a relaxed control policy, which results in low energy consumption and less wear and tear. The controller only reacted aggressively when it hit the boundaries of the safe operation zone. Hence the GNMPC can be implemented on applications where extreme levels of accuracy is not required. However, GNMPC is not suitable for large position setpoint changes. NMPC delivers the best performance in large setpoint changes with lower energy compared to the benchmark PID controller. In a situation where setpoint tracking is necessary, the GNMPC can be switched to a NMPC seamlessly by changing the weights in the objective function to constant values.

Another observation made during the experiment is the impact of the model accuracy on the performance of the NMPCs. The benchmark PID controller does not need any numerical model for the operation. However, the NMPCs highly depend on the accuracy of the numerical model. When the prediction horizon of the NMPCs is short, then the impact of an accurate model is minimal. However, when the prediction horizon is longer, the performance degrades significantly if the numerical model does not represent the actual vessel dynamics. Therefore, it is critical to validate the accuracy of the numerical model by conducting several test maneuvers.

The NMPC and GNMPC use optimization to calculate the optimal control action at each time step. The computation time required by the optimizer to calculate the optimal control sequence is a key consideration when implementing an NMPC controller. An NMPC with a longer prediction horizon generally performs better than an NMPC with a shorter prediction horizon. However, when the prediction horizon is longer, the optimizer requires more computational time to solve for the control action. Therefore, careful consideration has to be given when determining the optimizer, sampling time, and the length of the prediction horizon.

Wave filter was a critical part, especially in the NMPC implementations. When the direct feedback of the vessel motion is given to the

NMPC, the controller attempts to over-compensate for the oscillatory motion due to the first-order wave motions. In order to filter out the oscillatory motion from the feedback, a well-tuned wave filter is required. In this study, we used a UKF based wave filter to filter out the first-order wave effects, and the filter was reasonably easy to tune.

CRedit authorship contribution statement

Osama Alagili: Writing – original draft, Methodology, Investigation, Formal analysis, Data curation. **Eranga Fernando:** Writing – review & editing, Writing – original draft, Methodology, Investigation, Formal analysis, Data curation, Conceptualization. **Salim Ahmed:** Writing – review & editing, Supervision, Methodology, Funding acquisition, Conceptualization. **Syed Intiaz:** Writing – review & editing, Supervision, Methodology, Investigation, Funding acquisition, Conceptualization. **Kevin Murrant:** Writing – review & editing, Resources, Investigation, Data curation. **Bob Gash:** Writing – review & editing, Resources, Investigation, Data curation. **Mohammed Islam:** Writing – review & editing, Supervision, Resources, Project administration, Methodology, Data curation, Conceptualization. **Hasanat Zaman:** Writing – review & editing, Supervision, Resources, Project administration, Funding acquisition, Data curation.

Declaration of competing interest

The authors declare that they have no known competing financial interests or personal relationships that could have appeared to influence the work reported in this paper.

Data availability

Data will be made available on request.

Acknowledgment

This research was funded by National Research Council (NRC) of Canada under the funding agreement OCN-200-5. The authors gratefully acknowledge the support.

Appendix A. Supplementary data

Supplementary material related to this article can be found online at <https://doi.org/10.1016/j.oceaneng.2024.117297>.

References

- Alagili, O., Khan, M.A.I., Ahmed, S., Imtiaz, S., Zaman, H., Islam, M., 2022. An energy-efficient dynamic positioning controller for high sea conditions. *Appl. Ocean Res.* 129, 103331.
- Alfheim, H.L., Mugerud, K., Breivik, M., Brekke, E.F., Eide, E., Engelhardt, Ø., 2018. Development of a dynamic positioning system for the revolt model ship. *IFAC-PapersOnLine* 51 (29), 116–121.
- Andersson, J.A.E., Gillis, J., Horn, G., Rawlings, J.B., Diehl, M., 2019. CasADi – A software framework for nonlinear optimization and optimal control. *Math. Program. Comput.* 11 (1), 1–36. <http://dx.doi.org/10.1007/s12532-018-0139-4>.
- Balchen, J.G., Jenssen, N.A., Mathisen, E., Saelid, S., 1980. Dynamic positioning of floating vessels based on Kalman filtering and optimal control. In: 1980 19th IEEE Conference on Decision and Control Including the Symposium on Adaptive Processes. IEEE, pp. 852–864.
- Brodtkorb, A.H., Værnø, S.A., Teel, A.R., Sørensen, A.J., Skjetne, R., 2018. Hybrid controller concept for dynamic positioning of marine vessels with experimental results. *Automatica* 93, 489–497.
- Cavaleri, L., Alves, J.H., Arduin, F., Babanin, A., Banner, M., Belibassakis, K., Benoit, M., Donelan, M., Groeneweg, J., Herbers, T., et al., 2007. Wave modelling—the state of the art. *Prog. Oceanogr.* 75 (4), 603–674.
- Deng, F., Yang, H.L., Wang, L.J., 2019. Adaptive unscented Kalman filter based estimation and filtering for dynamic positioning with model uncertainties. *Int. J. Control Autom. Syst.* 17, 667–678.
- Diehl, M., Bock, H., Diedam, H., Wieber, P.B., 2006. Fast direct multiple shooting algorithms for optimal robot control. In: Diehl, M., Mombaur, K. (Eds.), *Fast Motions in Biomechanics and Robotics: Optimization and Feedback Control*. Springer Berlin Heidelberg, Berlin, Heidelberg, pp. 65–93. http://dx.doi.org/10.1007/978-3-540-36119-0_4.
- Du, J., Hu, X., Krstić, M., Sun, Y., 2016. Robust dynamic positioning of ships with disturbances under input saturation. *Automatica* 73, 207–214.
- Eriksen, B.-O.H., Breivik, M., 2017. Modeling, identification and control of high-speed ASVs: Theory and experiments. In: *Sensing and Control for Autonomous Vehicles: Applications to Land, Water and Air Vehicles*. Springer, pp. 407–431.
- Fannemel, Å.V., 2008. Dynamic Positioning by Nonlinear Model Predictive Control. Institutt for teknisk kybernetikk.
- Fossen, T.I., 2002. Marine control systems—guidance, navigation, and control of ships, rigs and underwater vehicles. In: *Marine Cybernetics*. www.marinecybernetics.com, Trondheim, Norway, Org. Number NO 985 195 005 MVA.
- Fossen, T.I., Sagatun, S.I., Sørensen, A.J., 1996. Identification of dynamically positioned ships. *Control Eng. Pract.* 4 (3), 369–376.
- Fossen, T.I., Strand, J.P., 1999. Passive nonlinear observer design for ships using Lyapunov methods: full-scale experiments with a supply vessel. *Automatica* 35 (1), 3–16.
- Grimble, M.J., Patton, R.J., Wise, D., 1980. The design of dynamic ship positioning control systems using stochastic optimal control theory. *Optim. Control Appl. Methods* 1 (2), 167–202.
- Grüne, L., Pannek, J., 2017. Economic NMPC. In: *Nonlinear Model Predictive Control: Theory and Algorithms*. Springer International Publishing, Cham, pp. 221–258. http://dx.doi.org/10.1007/978-3-319-46024-6_8.
- Hou, X., Deng, F., Yang, H., Yu, D., Zhang, H., Li, B., 2022. Robust nonlinear model predictive control for ship dynamic positioning using laguerre function. *IEEE Access* 10, 127563–127574.
- Hvamb, O.G., 2001. A new concept for fuel tight DP control. In: *Dynamic Positioning Conference*.
- Jayasiri, A., Nandan, A., Imtiaz, S., Spencer, D., Islam, S., Ahmed, S., 2017. Dynamic positioning of vessels using a UKF-based observer and an NMPC-based controller. *IEEE Trans. Autom. Sci. Eng.* 14 (4), 1778–1785.
- Johansen, T.A., Brekke, E., 2016. Globally exponentially stable Kalman filtering for SLAM with AHRS. In: 2016 19th International Conference on Information Fusion. FUSION, IEEE, pp. 909–916.
- Julier, S.J., Uhlmann, J.K., 1997. New extension of the Kalman filter to nonlinear systems. In: *Signal Processing, Sensor Fusion, and Target Recognition VI*, vol. 3068, Spie, pp. 182–193.
- Miller, P.A., Farrell, J.A., Zhao, Y., Djapic, V., 2010. Autonomous underwater vehicle navigation. *IEEE J. Ocean. Eng.* 35 (3), 663–678.
- Nguyen, T.D., Sørensen, A.J., Quek, S.T., 2007. Design of hybrid controller for dynamic positioning from calm to extreme sea conditions. *Automatica* 43 (5), 768–785.
- Pedersen, A.A., 2019. Optimization Based System Identification for the MilliAmpere Ferry (Master's thesis). NTNU.
- Rabanal, O.M., Brodtkorb, A.H., Breivik, M., 2016. Comparing controllers for dynamic positioning of ships in extreme seas. *IFAC-PapersOnLine* 49 (23), 258–264.
- Saelid, S., Jenssen, N., Balchen, J., 1983. Design and analysis of a dynamic positioning system based on Kalman filtering and optimal control. *IEEE Trans. Automat. Control* 28 (3), 331–339.
- Sørensen, A.J., 2011. A survey of dynamic positioning control systems. *Ann. Rev. Control* 35 (1), 123–136.
- Sørensen, A.J., Sagatun, S.I., Fossen, T.I., 1996. Design of a dynamic positioning system using model-based control. *Control Eng. Pract.* 4 (3), 359–368.
- Sorensen, A., Strand, J.P., Nyberg, H., 2002. Dynamic positioning of ships and floaters in extreme seas. In: *OCEANS'02 MTS/IEEE*, Vol. 3. IEEE, pp. 1849–1854.
- Sotnikova, M.V., Veremey, E.I., 2013. Dynamic positioning based on nonlinear MPC. *IFAC Proc. Vol.* 46 (33), 37–42.
- Tannuri, E.A., Morishita, H.M., 2006. Experimental and numerical evaluation of a typical dynamic positioning system. *Appl. Ocean Res.* 28 (2), 133–146.
- Torsetnes, G., Jouffroy, J., Fossen, T.I., 2004. Nonlinear dynamic positioning of ships with gain-scheduled wave filtering. In: 2004 43rd IEEE Conference on Decision and Control (CDC)(IEEE Cat. No. 04CH37601), Vol. 5. IEEE, pp. 5340–5347.
- Vekslar, A., Johansen, T.A., Borrelli, F., Realfsen, B., 2016. Dynamic positioning with model predictive control. *IEEE Trans. Control Syst. Technol.* 24 (4), 1340–1353.
- Wang, Y., 2006. Application of Model Predictive Control to Dynamic Positioning System (Master thesis). Harbin Engineering University.
- Wang, Y., Sui, Y., Wu, J., Jiao, J., 2012. Research on nonlinear model predictive control technology for ship dynamic positioning system. In: 2012 IEEE International Conference on Automation and Logistics. IEEE, pp. 348–351.
- Wei, X., Zhang, H., Wei, Y., 2022. Composite hierarchical anti-disturbance control for dynamic positioning system of ships based on robust wave filter. *Ocean Eng.* 262, 112173.
- Xu, S., Wang, X., Yang, J., Wang, L., 2020. A fuzzy rule-based PID controller for dynamic positioning of vessels in variable environmental disturbances. *J. Mar. Sci. Technol.* 25, 914–924.